ISSN 1027-5495. Functional Materials, 33, No.3 (2026), p. 462-474
doi:http://dx.doi.org/10.15407/fm33.03.462 © 2026 — SSI "Institute for Single Crystals"
This is an open access article under the CC BY-NC-ND license (http://creativecommons.org/licenses/by-nc-nd/4.0/).

Structure–property relationships and barrier performance of graphene oxide-reinforced epoxy–acrylate coatings for aggressive environments

Rana Khankishiyeva [1,2,3]*, Fariz Amirli[4], Turkan Mahmudova[5], Aynur Mammadova[6], Vugar Khudaverdiev[1,7], Ali Mammadov[1,3], Gunel Mammadova[1], Akif Salehov[1], Sanam Valiyeva[1], Reyhan Aliyeva[5,8], Aida Azizova[1], Narmin Mammadova[8], Haji Vahid Akhundzada[1,3,9]

[1]Institute of Physics, Ministry of Science and Education of the Republic of Azerbaijan, Baku AZ1143, Azerbaijan
[2]Department of Physics and Chemistry, Azerbaijan University of Architecture and Construction, Baku AZ1073, Azerbaijan
[3]Scientific - Research Institute «Geotechnological Problems of Oil, Gas and Chemistry», Azerbaijan State Oil and Industry University, Baku AZ1010,
[4] Institute of Polymer Materials, 147 Samad Vurgun Street, Sumgayit, AZ5004, Azerbaijan
[5]Department of Technology of Organic Substances and High Molecular Compounds, Azerbaijan State Oil and Industry University, Baku AZ1010, Azerbaijan
[6]Department of Process Safety Engineering, Azerbaijan State Oil and Industry University, Baku AZ1010, Azerbaija
[7]National Aviation Academy of Azerbaijan Airlines, Mardakan Ave. 30, Baku AZ1045, Azerbaijan
[8]Institute of Petrochemical Processes named after Academician Y. H. Mammadaliyev, Ministry of Science and Education the Republic of Azerbaijan, Baku AZ1025, Azerbaijan
[9]Industrial Chemistry Research Laboratory (ICRL), Baku State University, 23 Z. Khalilov Street, Baku AZ1148, Azerbaijan
*Corresponding author e-mail: renanamazova0@gmail.com

Received June 24, 2026, aproved August 12, 2026

Epoxy–acrylate GO-reinforced coatings reinforced with graphene oxide (GO) were developed to improve barrier performance in aggressive environments. GO nanosheets (1–3 wt.%) were incorporated into the polymer matrix using a controlled dispersion approach, followed by thermal curing to obtain crosslinked coatings. Thermal analysis showed enhanced stability: the 5% mass loss temperature ($T_{5\%}$) increased from 305 °C for pure epoxy resin to 320 °C for GO-modified systems, and the char residue also increased. Dynamic mechanical analysis

revealed higher stiffness and a shift of the glass transition toward lower temperatures, indicating the formation of a heterogeneous network structure. Mechanical testing demonstrated a decrease in tensile strength (28.3 to 23.8 MPa) and elongation, while hardness increased significantly (from 81.3 to 95.7 Shore units) and curing shrinkage was reduced. Chemical resistance was significantly improved: absorption in acidic environments decreased from 28% to ~15.9%, while even lower values were observed in alkaline and saline environments. These improvements are attributed to interfacial interactions between GO and the polymer matrix and the formation of a tortuous diffusion pathway that limits the transport of aggressive species. Overall, the results demonstrate that optimized GO incorporation enhances the durability and barrier properties of epoxy–acrylate coatings, despite a reduction in mechanical ductility at higher loadings.

Keywords: Epoxy–acrylate coatings; graphene oxide; nanocomposites; barrier properties; chemical resistance; thermal stability

Зв'язки між структурою та властивостями та бар'єрні характеристики епоксидно-акрилатних покриттів, армінованих оксидом графену, для агресивних середовищ. *Rana Khankishiyeva, Fariz Amirli, Turkan Mahmudova, Aynur Mammadova, Vugar Khudaverdiev, Ali Mammadov, Gunel Mammadova, Akif Salehov, Sanam Valiyeva, Reyhan Aliyeva, Aida Azizova, Narmin Mammadova, Haji Vahid Akhundzada*

Було розроблено епокси-акрилатні покриття, армовані оксидом графену (GO), для покращення бар'єрних властивостей в умовах дії агресивних середовищ. Нанолисти GO (1–3 мас. %) вводили в полімерну матрицю за допомогою методу контрольованого диспергування з подальшим термічним затвердінням для отримання зшитих покриттів. Термічний аналіз продемонстрував підвищену стабільність: температура втрати 5% маси (T_5%) зросла з 305 °C для вихідної епоксидної смоли до 320 °C для систем, модифікованих GO; також збільшився вихід коксового залишку. Динамічний механічний аналіз виявив підвищену жорсткість і зміщення температури склування в бік нижчих значень, що свідчить про формування гетерогенної сітчастої структури. Механічні випробування показали зниження міцності на розрив (з 28,3 до 23,8 МПа) та подовження при розриві, тоді як твердість суттєво зросла (з 81,3 до 95,7 одиниць за шкалою Шора), а усадка під час затвердіння зменшилася. Хімічна стійкість значно покращилася: приріст маси в кислому середовищі знизився з 28% до ~15,9%, причому ще нижчі показники спостерігалися в лужних і сольових середовищах. Такі покращення зумовлені міжфазною взаємодією між GO та полімерною матрицею, а також утворенням звивистого шляху дифузії, що обмежує проникнення агресивних речовин. Загалом результати свідчать про те, що оптимізоване введення GO підвищує довговічність і бар'єрні властивості епокси-акрилатних покриттів, попри зниження механічної пластичності при вищому вмісті наповнювача.

1. Introduction

Protective coating materials play a critical role in extending the service life of structural and engineering components by protecting surfaces against corrosion, mechanical degradation, and aggressive environmental conditions. In most coating systems, oligomeric resins serve as the primary film-forming component, determining key functional properties such as adhesion, elasticity, hardness, chemical resistance, and long-term durability (Gorninski et al., 2007; Agavriloaie et al., 2012) . Due to their tunable chemical structure and compatibility with various additives, oligomer-based coatings have become widely used in both conventional and advanced surface protection technologies.

Among the different classes of oligomers used in coating formulations, epoxy, acrylic, polyurethane, polyester and alkyd systems are the most extensively utilized. In particular, epoxy-based coatings are well known for their excellent adhesion to various substrates, high mechanical strength, and superior resistance to chemical and corrosive environments (Jin et al., 2015). These properties make epoxy resins highly suitable for applications in industrial flooring, protective coatings for metal structures, storage systems, and chemically aggressive environments. However, despite these advantages, conventional epoxy coatings often suffer from inherent limitations, including brittleness, sensitivity to ultraviolet radiation, and the formation of microdefects during curing. These microvoids and defects facilitate the penetration of water, oxygen, and aggressive ions, ultimately reducing the long-term protective performance of the coating (Liu et al., 2021; Sanya & Panesar, 2026).

To solve these problems, chemical modification of epoxy resins has become an effective strategy. One of the most promising approaches involves the introduction of acrylate functional groups, leading to the formation of epoxy–acrylate oligomers. These systems combine the excellent adhesion and chemical resistance of

epoxy resins with the rapid curing capability and surface hardness associated with acrylate polymers. As a result, epoxy–acrylate coatings exhibit improved curing kinetics, enhanced crosslink density, and better resistance to aggressive chemical media (Müller et al., 2020). Such nanocomposite coating systems are particularly attractive for applications requiring both high performance and processing efficiency.

In parallel, the incorporation of nanostructured fillers into polymer matrices has attracted increasing attention as a powerful approach to further enhance coating performance. Among various nanofillers, graphene-based materials, particularly reduced graphene oxide (GO), have proven to be very promising candidates due to their exceptional mechanical strength, high aspect ratio, and outstanding impermeability. The incorporation of GO nanosheets into polymer coatings has been shown to significantly improve barrier properties by creating a highly tortuous diffusion pathway, thereby limiting the transport of corrosive species such as water, oxygen, and ions (Jia & Zhang, 2024).

Several studies have demonstrated the effectiveness of GO in improving the performance of epoxy-based coatings. For example, Fan et al. (2019) reported that GO-modified epoxy–acrylate systems can reduce corrosion rates by several orders of magnitude. Similarly, Cao et al. (2015) observed a reduction of more than 97% in corrosion rate for GO-reinforced coatings compared to neat polymers. Xie et al. (2020) further demonstrated a significant increase in impedance modulus, indicating enhanced barrier efficiency and coating integrity. These improvements are mainly attributed to the formation of a multi-layered nanosheet structure within the polymer matrix, which effectively blocks diffusion pathways and enhances the overall resistance of the coating.

Despite these promising results, the practical application of GO in polymer coatings remains challenging due to its strong tendency to agglomerate as a result of van der Waals interactions. Poor dispersion of GO nanosheets can lead to structural heterogeneities, defect formation, and even localized corrosion phenomena, ultimately limiting the effectiveness of the nanofiller (Selim et al., 2024; Thorshaug et al., 2024). Therefore, achieving uniform dispersion and strong interfacial interaction between GO and the polymer matrix is essential for maximizing its reinforcing potential.

In this context, the present study focuses on the synthesis of epoxy oligomers based on bisphenol A and epichlorohydrin, followed by their modification into epoxy–acrylate oligomer systems. Furthermore, GO-reinforced nanocomposite coatings were prepared using a controlled dispersion approach. The study aims to investigate the structure–property relationships governing the performance of these coatings, with particular emphasis on barrier properties, thermal stability, and resistance to aggressive chemical environments. The findings are expected to provide valuable insights into the design of high-performance graphene-based protective coatings for advanced engineering applications.

2. Experimental

2.1 Materials

Bisphenol A (BPA, ≥99%), epichlorohydrin (ECH, ≥99%), sodium hydroxide (NaOH, 50 wt% aqueous solution), methacrylic acid (MAA, ≥99%), and toluene (analytical grade) were purchased from Sigma-Aldrich and used without further purification. Distilled water was used throughout the experimental procedures. Graphene oxide (GO) was synthesized in-house and used as a nanofiller in the preparation of nanocomposite coatings. Cymel® 325 (hexamethoxymethyl melamine, HMMM, Allnex, Germany) was used as the curing agent for the epoxy–acrylate coating formulations.

2.1.2 Synthesis of Graphene Oxide (GO)

Graphene oxide (GO) was synthesized using a modified Hummers method according to previously reported procedures (Guerrero-Contreras and Caballero-Briones, 2015; Sujiono et al., 2020). In a typical synthesis, 3.0 g of graphite powder and 1.5 g of sodium nitrate ($NaNO_3$) were mixed, followed by the slow addition of 70 mL of concentrated sulfuric acid (H_2SO_4) under continuous stirring in an ice bath (0 °C) for 1 h. Subsequently, 9.0 g of potassium permanganate ($KMnO_4$) was added gradually while maintaining the temperature below 20 °C. The reaction mixture was kept at 0 °C for 3 h and then stirred at 35 °C for an additional 1 h. Distilled water (150 mL) was added dropwise, resulting in an exothermic reaction with the temperature rising to approximately 98 °C. The system was maintained at this temperature for 30 min, followed by the addition of 300 mL of distilled water.

Residual manganese species were reduced by adding 15 mL of 30% hydrogen peroxide (H_2O_2) until the color changed to yellow. The product was filtered and washed with diluted hydrochloric acid (HCl:water = 1:10), followed by repeated washing with distilled water until neutral pH was achieved. The obtained GO was dried at room temperature, redispersed in water using ultrasonication (150 W, 40 kHz), and centrifuged to obtain a stable dispersion.

Previous characterization of graphene oxide prepared under identical synthesis conditions by our research group using TEM and AFM revealed a layered morphology with exfoliated graphene oxide nanosheets (Tene et al., 2026). The XRD results obtained in the present study are consistent with these observations, confirming the successful oxidation and exfoliation of graphite during GO preparation.

2.1.3 Synthesis of Epoxy Oligomer

The epoxy oligomer was synthesized via the reaction of bisphenol A (BPA) with epichlorohydrin (ECH) under alkaline conditions. Initially, epichlorohydrin (25 mL) was introduced into the reactor, followed by the addition of 5 g of BPA. The mixture was heated to 90–100 °C under continuous stirring to ensure complete dissolution of BPA. After achieving a homogeneous solution, the temperature was reduced to 60 °C. A 50 wt% NaOH solution was then added dropwise (4 mL) under continuous stirring. The reaction was maintained at 60 °C for 4 h. Under alkaline conditions, phenolic hydroxyl groups of BPA were converted into phenoxide ions, which reacted with epichlorohydrin via nucleophilic substitution. This resulted in the formation of chlorohydrin intermediates, followed by intramolecular cyclization to form epoxy (oxirane) groups. The final product was primarily diglycidyl ether of bisphenol A (DGEBA), with a degree of oligomerization dependent on the ECH/BPA ratio.

After completion of the reaction, the mixture was transferred into a separatory funnel for phase separation. The aqueous phase was removed, and the organic phase was collected.

The product was washed 2–3 times with distilled water to remove residual alkali and by-products. Subsequently, the epoxy oligomer was dried at 50 °C for 1 h. A light yellow, viscous, and homogeneous epoxy oligomer was obtained, confirming successful synthesis.

The epoxy equivalent weight (EEW) of the synthesized epoxy oligomer was determined according to ASTM D1652 and was approximately 187 g/eq. Assuming a bifunctional DGEBA structure containing two epoxy groups per molecule, the corresponding average molecular weight was estimated to be about 374 g/mol. These values are consistent with those reported for low-molecular-weight DGEBA-based epoxy oligomers.

2.1.4 Synthesis of Epoxy–Acrylate Oligomer

The epoxy oligomer was modified using methyl metacrylate (MMA) to introduce an acrylate functional group. Briefly, 10 g of epoxy oligomer was dissolved in 10 mL of toluene and stirred at room temperature (≈25 °C) for 30 min. Then, 1 g of MMA was added, and the mixture was stirred for an additional 30 min. The reaction proceeded by opening the epoxy ring with the carboxyl groups of MMA, resulting in the formation of ß-hydroxy ester linkages and incorporation of vinyl groups into the polymer structure. The reaction proceeded under mild conditions without additional catalysts, likely facilitated by the intrinsic reactivity of epoxy groups.

2.1.5 Preparation of Epoxy–Acrylate/GO Nanocomposites

Epoxy–acrylate/GO nanocomposites were prepared using a solvent-assisted dispersion method. GO (0.2–0.4 g, corresponding to 2–4 wt%) was dispersed in 10 mL of toluene using an ultrasonic bath (150 W, 40 kHz) for 45 min. The selected frequency provided effective and homogeneous dispersion of GO nanosheets while minimizing excessive fragmentation, whereas the sonication time was optimized through preliminary experiments to obtain stable dispersions with reduced agglomeration.

Separately, 10 g of epoxy–acrylate oligomer was dissolved in toluene under mechanical stirring at room temperature for 30 min. The GO dispersion was then gradually added under continuous stirring. The mixture was stirred for 30 min and subsequently subjected to an additional 15 min of ultrasonication to ensure uniform distribution of GO within the oligomer matrix. Finally, 3 g of melamine curing agent (pre-dissolved in toluene) was added, and the mixture was stirred for a further 10–15 min before coating application.

2.1.6 Coating application and curing

The prepared compositions were applied onto pre-cleaned glass and steel substrates using a drop-casting method. Glass substrates

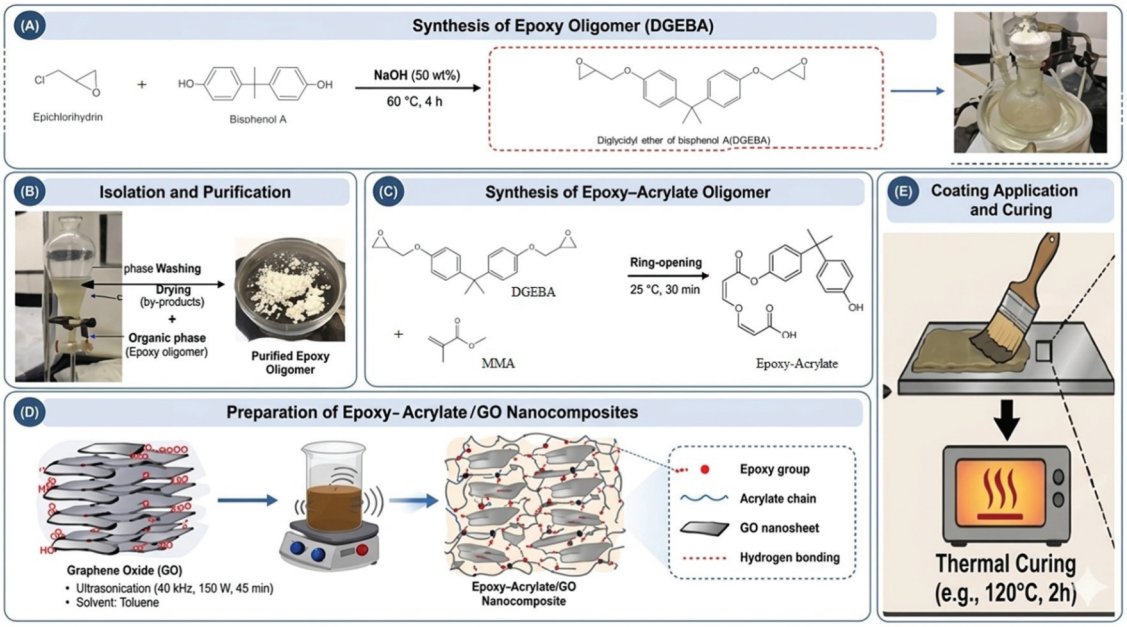

Fig.1. Process flow diagram illustrating the preparation of epoxy–acrylate/GO nanocomposites, including raw material processing, purification, matrix modification, nanofiller dispersion, and final coating and curing stages.

were used for FTIR, optical, and morphological characterization, whereas steel panels were employed for mechanical, adhesion, and chemical resistance tests. Prior to coating, all substrates were cleaned with ethanol and distilled water. The coatings were kept at room temperature (25 °C) for 24 h to ensure solvent evaporation and were subsequently cured at 100 °C for 4–5 h in a laboratory oven. The resulting coatings exhibited an average dry film thickness of 50–80 μm, measured using an Elcometer coating thickness gauge. After curing, the samples were cooled to room temperature before characterization.

2.2. Methods

2.2.1 FTIR Spectroscopy

Fourier transform infrared (FTIR) spectra were recorded in the range of 4000–600 cm^{-1} with a spectral resolution of 4 cm^{-1} and 32 scans per sample. Background spectra were collected prior to each measurement and automatically subtracted. Cured coating samples were analyzed directly after cleaning with ethanol and drying under ambient conditions.

2.2.2. Structural and Morphological Characterization

X-ray diffraction (XRD) analysis was carried out using a Rigaku MiniFlex 600 diffractometer with Cu Kα radiation (λ = 1.5406 Å) in the 2θ range of 5–80 degrees to investigate the structural features of GO and its dispersion within the polymer matrix.

Surface morphology and dispersion of GO nanosheets were examined using scanning electron microscopy (SEM) (JEOL JSM-6490LV and TESCAN VEGA) at an accelerating voltage of 20 kV. Energy-dispersive X-ray spectroscopy (EDS) was used for elemental analysis and to confirm the distribution of GO within the composite.

2.2.3. Thermal Analysis (TGA and DSC)

Thermal stability of the coatings was evaluated using thermogravimetric analysis (TGA). Measurements were performed under nitrogen atmosphere from room temperature to 800 °C at a heating rate of 10 °C/min.

Key parameters such as initial degradation temperature ($T_{5\%}$), maximum degradation temperature (T_{max}), and residual mass were determined to assess thermal stability.

Differential scanning calorimetry (DSC) was used to investigate thermal transitions, including glass transition temperature (T_g). Samples were heated from room temperature to 250 °C at a rate of 10 °C/min under nitrogen atmosphere.

2.2.4. Mechanical, adhesion, and chemical resistance properties

Mechanical properties of the coatings were evaluated in terms of tensile strength, elongation at break, hardness, and adhesion. Tensile

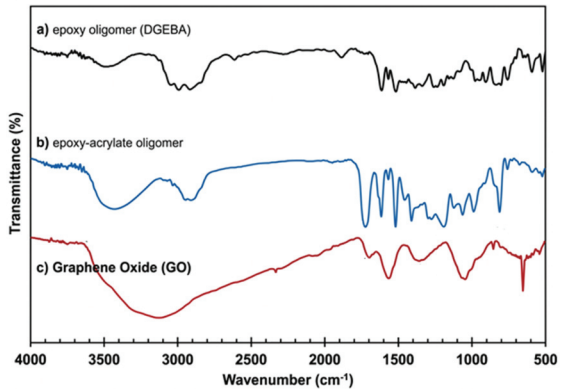

Figure 2. FTIR spectra of the synthesized precursor materials: (a) DGEBA epoxy oligomer, (b) epoxy–acrylate oligomer, and (c) graphene oxide (GO).

measurements were performed using a universal testing machine (ZwickRoell Z020) according to ISO 37:2017 at a crosshead speed of 500 mm/min. Hardness was determined using a Shore A durometer in accordance with ISO 7619-1:2010. Adhesion strength to metal substrates was evaluated following ASTM D429 Method B. Impact resistance and flexibility were assessed using a paint film impact tester (QCJ, Tianjin, China) and a pendulum hardness tester (QHB, Tianjin, China), respectively.

Chemical resistance was evaluated by immersing the coated specimens in 40% KOH, 28% H_2SO_4, and 3% artificial seawater solutions at room temperature for 21 days. After exposure, the samples were removed, rinsed, dried to constant weight, and the percentage mass change was determined.

3. Results and discussion

3.1 FTIR Analysis

FTIR spectroscopy was used to follow the chemical evolution of the system from the initial epoxy oligomer to the epoxy–acrylate oligomer structure and subsequently to the GO-modified epoxy–acrylate coatings. FTIR analysis was performed to confirm the successful synthesis of DGEBA, epoxy–acrylate oligomer, and graphene oxide, as well as their incorporation into the coating compositions. The spectra presented in Fig. 2 and Fig. 3 provide a consistent picture of these structural transformations.

The spectrum of the neat epoxy oligomer shows the expected features of a DGEBA-type structure. In particular, the absorption band at around 910–915 cm^{-1}, assigned to the oxirane ring vibration, clearly confirms the presence of epoxy groups. The aromatic backbone is reflected in the bands located in the 1500–1600 cm^{-1} region, while the broad signal around 3400 cm^{-1} is associated with hydroxyl groups, which are commonly present due to partial ring opening or residual functional groups in the system.

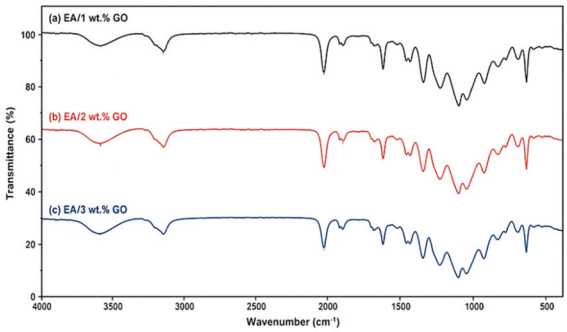

Fig.3. FTIR spectra of epoxy–acrylate (EA) coatings containing (a) 1 wt.% GO, (b) 2 wt.% GO, and (c) 3 wt.% GO

After modification with methacrylic acid, the changes in the spectrum are quite revealing. The epoxy signal at ~910 cm^{-1} is noticeably weakened, which directly indicates that the the ring-opening reaction has occurred. At the same time, a new and relatively intense band appears at ~1720–1730 cm^{-1}, corresponding to the ester carbonyl group. This is a key indicator that the epoxy–acrylate structure has been successfully formed. The weak feature observed near ~1635 cm^{-1} further supports the introduction of vinyl groups into the system.

The role of GO becomes clearer when comparing the spectra of the nanocomposite matrix with those of the nanocomposites (Fig. 3). As expected, GO itself exhibits broad hydroxyl absorption in the 3200–3500 cm^{-1} region, along with contributions from carbonyl and C–O functional groups. When GO is incorporated into the epoxy–acrylate matrix, this region becomes progressively broader with increasing GO content. This is not just a simple superposition effect; rather, it indicates the formation of hydrogen bonding interactions between the oxygen-containing groups of GO and the hydroxyl and ester groups of the polymer network.

A similar trend can be observed in the 1050–1250 cm^{-1} region, where overlapping C–O and C–O–C vibrations become more pronounced and slightly broadened. This behavior is typically associated with interfacial interactions and provides indirect evidence that GO is reasonably well integrated into the matrix rather than existing as a completely separate phase.

It is also worth noting that at higher GO loadings, some of the polymer-related bands become less sharp and slightly attenuated.

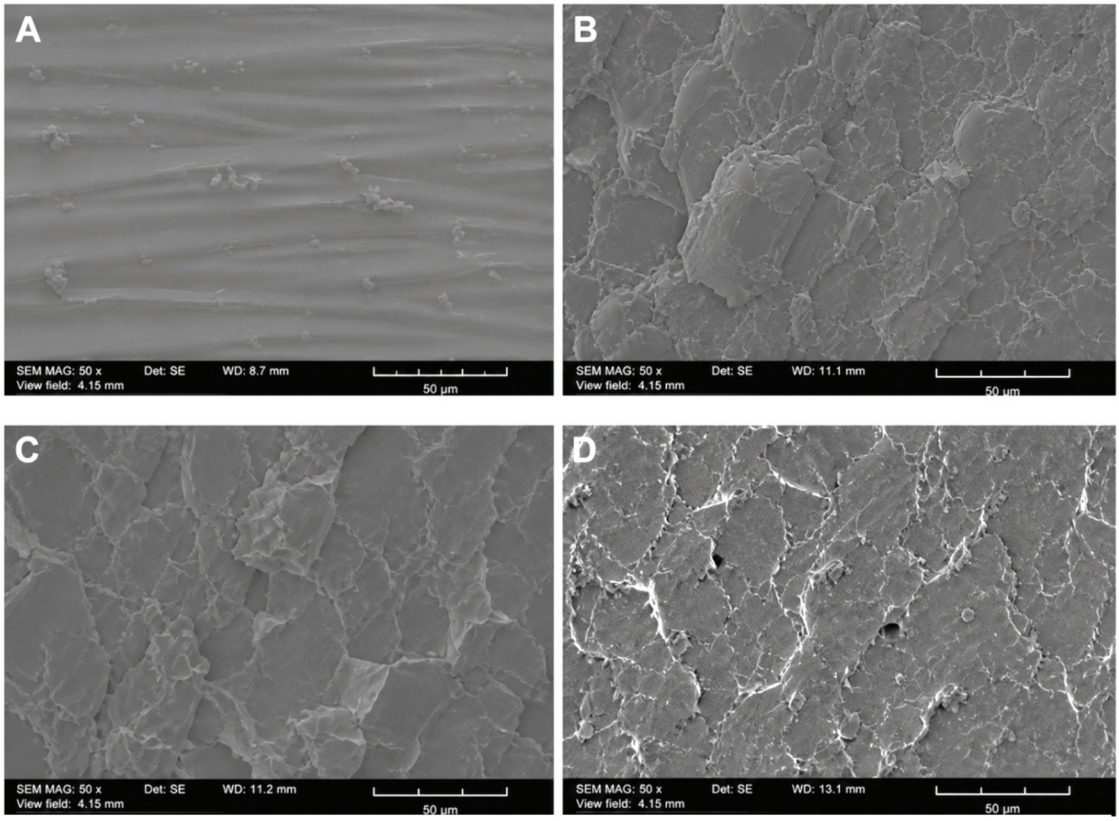

Fig. 4. SEM images of (a) neat epoxy–acrylate (EA) coating and EA coatings containing (b) 1 wt.% GO, (c) 2 wt.% GO, and (d) 3 wt.% GO.

This can be interpreted as a consequence of restricted chain mobility and increased structural heterogeneity at higher filler concentrations. In other words, while GO enhances interfacial interactions, excessive loading may begin to perturb the uniformity of the polymer network.

Taken together, the FTIR results confirm not only the successful formation of the epoxy–acrylate structure but also the active participation of GO in the system through interfacial interactions. These interactions are likely to play a central role in the improved barrier and chemical resistance properties observed in the subsequent sections.

3.2 Morphology and Dispersion (SEM and XRD Analysis)

The morphology and dispersion state of graphene oxide (GO) within the epoxy–acrylate (EA) matrix were investigated using scanning electron microscopy (SEM) and X-ray diffraction (XRD) analysis. These techniques provide complementary insights into the microstructural organization of the nanocomposites and the quality of filler distribution.

The SEM images presented in Fig. 4 reveal clear differences in surface morphology between the neat EA coating and GO-modified systems. The neat EA sample (Fig. 4a) exhibits a relatively smooth and continuous surface with visible microdefects and occasional irregularities, which are typical for thermally cured epoxy-based coatings. These microstructural imperfections can act as preferential pathways for the penetration of aggressive species.

Upon incorporation of GO, a noticeable change in morphology is observed. At low GO content (1 wt.%, Fig. 4b), the surface becomes more textured, indicating the presence of dispersed nanosheets within the polymer matrix. The GO sheets appear to be embedded within the matrix, contributing to a more compact structure. This suggests relatively good dispersion and interfacial compatibility at low loading levels.

At intermediate GO content (2 wt.%, Fig. 4c), the structure becomes more uniform and densely packed. The layered morphology becomes more apparent, indicating that GO nanosheets are distributed throughout the matrix and may form a partially interconnected network. This type of structure is beneficial for barrier performance, as it increases the tortuosity of diffusion pathways.

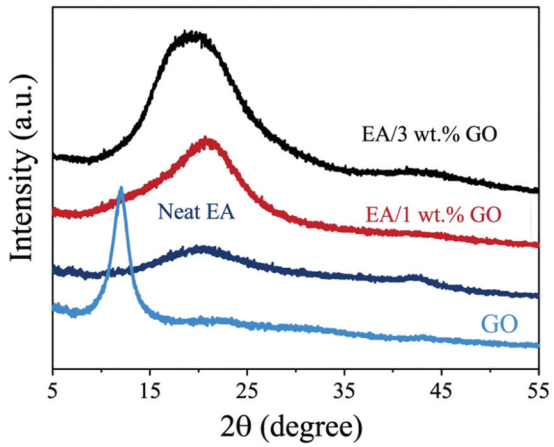

Fig. 5. XRD patterns of GO, neat epoxy–acrylate (EA), and EA/GO nanocomposites with different GO contents.

However, at higher GO loading (3 wt.%, Fig. 4d), signs of partial agglomeration begin to appear. Localized clusters and less homogeneous regions can be observed, together with the appearance of microvoids or stress-induced defects. Although ultrasonication effectively improved the initial dispersion of GO nanosheets, partial re-agglomeration may occur during solvent evaporation and thermal curing due to van der Waals interactions between neighboring sheets. As a result, a less uniform morphology is observed at higher GO concentrations.

Overall, the SEM observations indicate that GO is fairly well dispersed within the EA matrix at low to moderate concentrations, while excessive concentrations lead to reduced homogeneity.

XRD analysis (Fig. 5) further supports these findings by providing information on the structural arrangement of GO within the polymer matrix. The XRD pattern of pure GO shows a characteristic diffraction peak at low angles (around $2\theta \approx 10–12°$), corresponding to the (001) plane and indicating an ordered layered structure with increased interlayer spacing due to oxygen-containing functional groups.

In contrast, the neat EA matrix exhibits a broad amorphous halo, typical of crosslinked polymer systems lacking long-range crystalline order. Upon incorporation of GO, this characteristic GO peak is either significantly reduced in intensity or completely disappears in the nanocomposite samples. Instead, a broad diffraction feature is observed.

This disappearance or weakening of the GO peak suggests that the layered structure of GO is largely disrupted within the polymer matrix. Such behavior is commonly interpreted as evidence of exfoliation or good dispersion of GO nanosheets. The absence of a sharp diffraction peak indicates that GO layers are no longer stacked in an ordered manner but are instead separated and distributed within the matrix.

Additionally, slight changes in the position and intensity of the amorphous halo may indicate interactions between GO and the polymer chains, which can influence chain packing and local ordering.

Taken together, the SEM and XRD results provide consistent evidence that GO is effectively incorporated into the epoxy–acrylate matrix and that its dispersion state strongly depends on the loading level. At optimal concentrations, GO is well distributed and contributes to a more compact and tortuous microstructure, which is expected to enhance barrier and chemical resistance properties. However, at higher loadings, partial agglomeration reduces structural uniformity and may limit performance improvements.

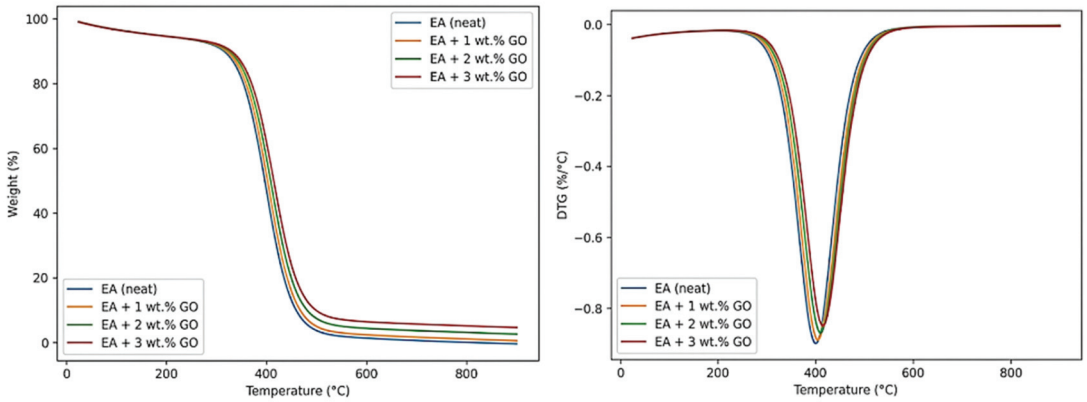

Fig. 6. TGA and DTG curves of neat epoxy (EA) and GO-reinforced composites containing 1–3 wt.% graphene oxide. (a) TGA curves showing the temperature-dependent weight loss behavior; (b) DTG curves illustrating the rate of thermal degradation as a function of temperature.

Table 1.The extracted degradation parameters

Sample	$T_{5\%}$ (°C)	$T_{10\%}$ (°C)	T_{max} (°C, DTG)	Residue at 800°C (%)
EA (neat)	305	330	395	1.2
EA + 1 wt.% GO	310	335	400	2.0
EA + 2 wt.% GO	315	340	405	3.5
EA + 3 wt.% GO	320	345	410	5.0

3.3. Thermogravimetric Analysis (TGA/DTG)

The thermal degradation behavior of neat epoxy (EA) and composites reinforced with graphene oxide (GO) was investigated by TGA, while DTG curves were used to resolve the kinetics of mass loss (Fig. 6 (a–b)).

All compositions exhibit a dominant single-step decomposition profile, indicating that the degradation process is governed primarily by the breakdown of the crosslinked epoxy network rather than by multiple independent mechanisms. The absence of significant mass loss below ~150 °C confirms the negligible presence of low-molecular-weight species and suggests a well-cured thermoset structure.

The onset of thermal degradation progressively shifts toward higher temperatures with increasing GO content, as reflected by the increase in $T_{5\%}$ and $T_{10\%}$ values (Table 1). This shift cannot be solely attributed to filler dilution; rather, it indicates that GO alters the heat transfer pathways and volatilization kinetics within the matrix.

The improved thermal stability can be attributed to the combined effect of the barrier function of layered GO nanosheets and the enhanced interfacial interactions between GO and the epoxy–acrylate network. The presence of GO restricts heat and mass transfer during thermal degradation, while strong interfacial interactions contribute to the stabilization of the polymer structure, resulting in a delay in the onset of thermal decomposition.

The DTG profiles (Fig. 6(b)) provide further mechanistic insight. Each sample exhibits a single, well-defined maximum degradation rate (T_{max}), supporting a predominantly homogeneous degradation pathway. However, a slight shift of T_{max} toward higher temperatures is observed upon GO incorporation, indicating improved thermal stability of the coating system. This behavior is consistent with restricted chain mobility and enhanced interfacial interactions between the epoxy network and GO sheets.

More importantly, the DTG peak shape changes depending on the filler content. The slight broadening observed for GO-containing samples indicates a distribution of local environments with different thermal resistances. This heterogeneity arises from interfacial regions where polymer chains are partially constrained by GO surfaces, leading to delayed and spatially non-uniform decomposition.

Figure 6(a) clearly shows a pronounced increase in residual mass at elevated temperatures, and a quantitative assessment is given in Table 1. The char yield increases systematically with GO loading, indicating that GO participates in the formation of a thermally stable carbonaceous framework. This effect can be rationalized by two concurrent mechanisms: (1) the catalytic promotion of char formation and (2) the physical shielding effect of GO layers, which reduce heat flux and limit oxidative degradation of the underlying matrix.

Taken together, these observations demonstrate that GO incorporation modifies not only the onset of degradation but also the degradation pathway itself. The combined increase in $T_{5\%}$, T_{max}, and char yield indicates a transition toward a more thermally robust system, where mass transport limitations and interfacial confinement play a central role in governing decomposition behavior.

3.3. Dynamic Mechanical Analysis (DMA)

The temperature dependences of storage modulus (E') and loss modulus (E'') for EA and GO-filled composites are shown in Fig. 7(a–b).

E' decreases with temperature for all samples, reflecting the glass–rubber transition. In the glassy region, stiffness of GO slightly increases due to restricted chain mobility at the polymer–filler interface. However, the transition region shifts toward lower temperatures with increasing GO content, indicating a reduction in effective crosslink density or the formation of interfacial free volume.

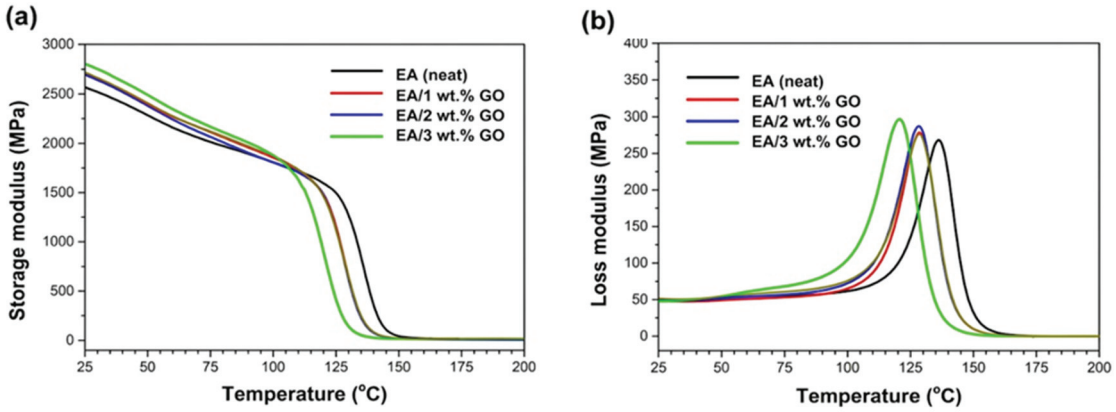

Fig. 7. Storage modulus (E') (a) and loss modulus (E'') (b) of neat epoxy (EA) and GO-reinforced composites as a function of temperature

The E'' curves exhibit a single α-relaxation peak associated with T_g. With GO addition, the peak shifts to lower temperatures and becomes broader, indicating enhanced segmental mobility along with increased structural heterogeneity. The increased peak intensity further indicates higher energy dissipation, attributed to interfacial friction between GO and the epoxy matrix.

The decrease in T_g observed by DMA, DMA, along with the increase in thermal stability revealed by TGA, indicates that GO forms a heterogeneous network structure. While interfacial regions around GO promote earlier segmental relaxation (lower T_g), the layered morphology simultaneously limits heat and mass transfer during degradation, resulting in higher $T_{5\%}$, T_{max}, and char yield. This apparent contradiction reflects the dual role of GO, acting both as a mobility modifier at the microscale and as a thermal barrier at elevated temperatures.

3.4. Physical–mechanical properties of EA/GO-based coating composites

The physical–mechanical and chemical properties of EA/GO coating composites are summarized in Table 2.

A systematic variation in the physical–mechanical properties of the coatings is observed with increasing GO content. Tensile strength gradually decreases with increasing filler content, which can be attributed to the formation of localized GO agglomerates acting as stress concentration sites and reducing the efficiency of stress transfer within the polymer matrix. A similar trend is observed for peel and shear adhesion to metal substrates.

Although GO enhances coating rigidity, excessive filler content may reduce interfacial compliance and promote the development of internal stresses during curing, leading to lower adhesion values. In contrast, hardness increases significantly (81.3–95.7 Shore units), reflecting the rigid nature of GO nanosheets and their ability to restrict polymer chain mobility. The decrease in elastic rebound further supports this observation, indicating reduced elasticity and increased stiffness of the coating network. At the same time, the reduction in curing shrinkage demonstrates improved dimensional stability, while the enhanced resistance to alkaline, acidic, and saline media confirms the beneficial barrier effect of GO within the epoxy–acrylate matrix.

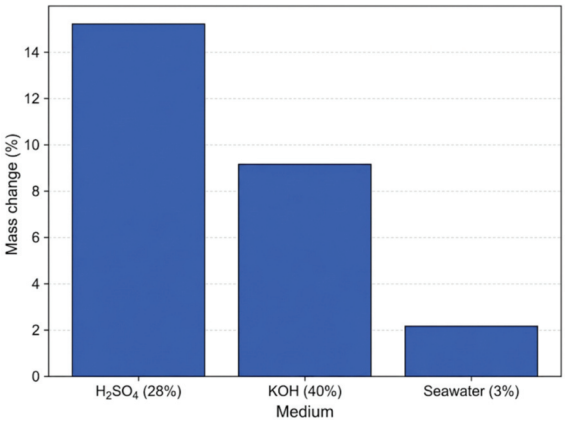

Fig. 8. Final mass change of EA/GO coating after exposure to acidic (H_2SO_4), alkaline (KOH), and saline (seawater) media

The reduction in curing shrinkage (1.6 → 0.7%) indicates improved dimensional stability, suggesting that GO effectively limits volumetric contraction during network formation. This behavior is consistent with the partial confinement of polymer chains within the filler–matrix interphase.

Adhesion behavior exhibits substrate-dependent trends. Adhesion to metal decreases

Table 2. Effect of graphene oxide (GO) content on the physical–mechanical performance and chemical resistance of epoxy–acrylate (EA) coating composites

No.	Property	EA (neat)	EA + 1 wt.% GO	EA + 2 wt.% GO	EA + 3 wt.% GO
1	Tensile strength, MPa	28.3	26.5	25.2	23.8
2	Elongation at break, %	34	35	33	29
3	Shrinkage during curing, %	1.6	1.4	1.1	0.7
4	Adhesion to metal (peel), MPa	7.8	7.0	6.3	4.8
5	Adhesion to metal (shear), MPa	8.3	7.4	6.4	5.0
6	Hardness (TM-2), Shore units	81.3	89.7	92.6	95.7
7	Elastic rebound, %	9.0	8.6	7.9	7.0
8	Adhesion to wood, MPa	7.7	8.02	9.05	9.7
9	Chemical resistance (40% KOH), % mass change	17.0	9.11	9.15	9.2
10	Chemical resistance (28% H2SO4), % mass change	28.0	15.2	15.7	15.9
11	Chemical resistance (3% seawater), % mass change	4.0	2.18	2.22	2.25

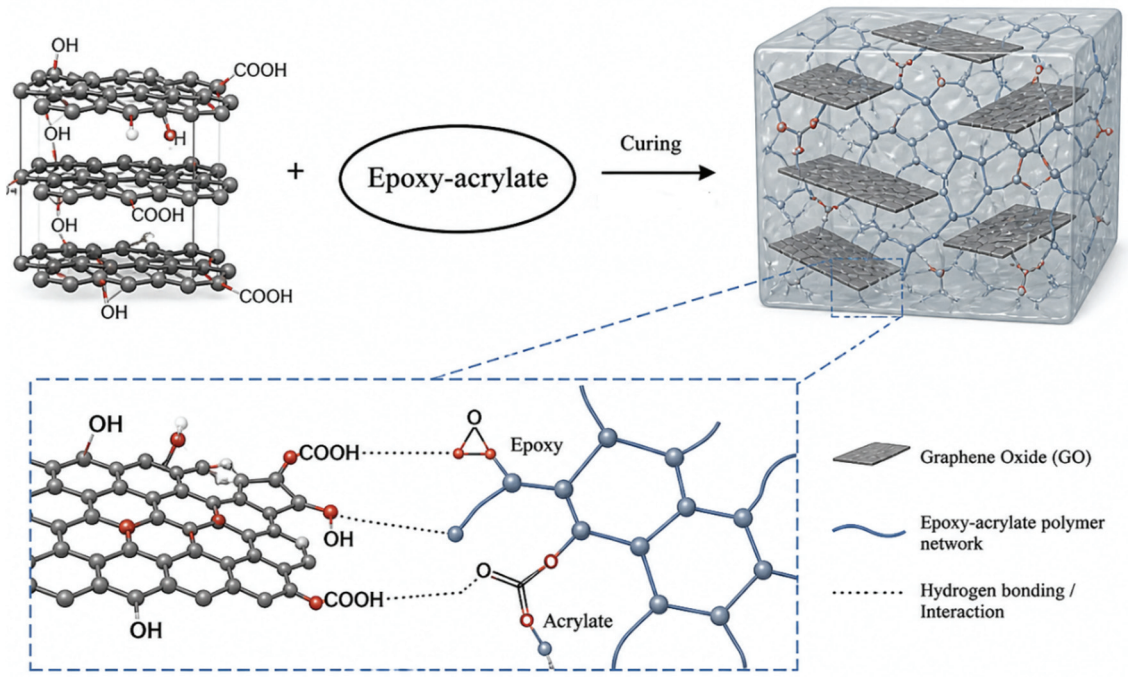

Fig.9. Schematic illustration of the interaction between graphene oxide (GO) and the epoxy–acrylate network, showing interfacial bonding and the formation of a tortuous diffusion pathway.

with GO content, which is likely due to increased stiffness and reduced interfacial compliance. Conversely, adhesion to wood improves (7.7 → 9.7 MPa), which may be attributed to enhanced mechanical interlocking and changes in surface energy induced by GO incorporation.

The most pronounced effect of GO is observed in chemical resistance. The significant reduction in mass uptake in aggressive media (e.g., H_2SO_4: 28% → ~15.9%) indicates suppressed diffusion of corrosive species. The final mass change of the coating after exposure to different aggressive media is shown in Fig. 8.

This improvement is associated with the formation of a tortuous diffusion pathway created by GO nanosheets, which effectively hinders the penetration of liquids into the polymer matrix. GO incorporation results in a trade-off between mechanical ductility and durability, where increased rigidity and reduced permeability enhance chemical resistance and dimensional stability.

3.5. Interaction mechanism of GO in epoxy–acrylate coating

The interaction mechanism of GO in the epoxy–acrylate network is shown in Fig. 9.

Oxygen-containing groups on GO (–OH, –COOH) form hydrogen bonds with the polymer matrix during curing. This creates a constrained interfacial region and limits chain mobility.

As a result, GO behaves as a physical crosslinking site, increasing hardness and stiffness. At the same time, the layered structure of GO forms a tortuous path that slows down the diffusion of aggressive species. This explains the reduced mass uptake observed in acidic, alkaline, and saline media.

However, at higher GO contents, partial agglomeration leads to stress concentration, which contributes to the decrease in tensile properties.

Conclusion

Graphene oxide-reinforced epoxy–acrylate coatings were successfully developed, and their structure–property relationships were systematically evaluated. The incorporation of GO enhanced thermal stability, hardness, and chemical resistance, as evidenced by increased degradation temperatures, higher char yield, and reduced mass uptake in aggressive media.

These improvements originate from interfacial interactions between GO and the polymer matrix and the formation of a tortuous diffusion pathway that limits the transport of corrosive species. At the same time, increasing GO content leads to reduced tensile strength and elongation due to agglomeration and stress concentration effects. The results demonstrate a clear trade-off between mechanical ductility and barrier performance, highlighting the importance of optimized GO content. Overall, the developed coatings show strong potential for applications requiring high chemical resistance and long-term durability in aggressive environments.

Reference

1. Gorninski, J.P., Dal Molin, D.C., Kazmierczak, C.S., 2007. Strength degradation of polymer concrete in acidic environments. *Cement and Concrete Composites* 29, 637–645.
2. Agavriloaie, L., Oprea, S., Barbuta, M., Luca, F., 2012. Characterisation of polymer concrete with epoxy polyurethane acryl matrix. *Construction and Building Materials* 37, 190–196.
3. Majid, M.S.A., Ridzuan, M.J.M., Lim, K.H., 2020. Effect of nanoclay filler on mechanical and morphological properties of napier/epoxy composites. *Woodhead Publishing Series in Composites Science and Engineering*, 137–162.
4. Ifijen, I.H., Udokpoh, N.U., Onaiwu, G.E., Jonathan, E.M., Ikhuoria, E.U., 2022. Coating properties of alkyd, epoxy, and polyurethane-based nanocomposites: A review. *Malaysian Journal of Fundamental and Applied Sciences* 14(1), 1–31.
5. Lichołai, L., Dębska, B., 2014. Effect of corrosive solutions on physical properties of modified epoxy mortars. *Construction and Building Materials* 65, 604–611.
6. Jin, F.L., Li, X., Park, S.J., 2015. Synthesis and application of epoxy resins: A review. *Journal of Industrial and Engineering Chemistry* 29, 1–11.
7. Jeon, H., Park, J., Shon, M., 2013. Corrosion protection by epoxy coatings containing multi-walled carbon nanotubes. *Journal of Industrial and Engineering Chemistry* 19(3), 849–853.
8. Müller, M.T., Zschech, C., Gedan-Smolka, M., Pech, M., Streicher, R., Gohs, U., 2020. Surface modification and edge layer post curing of sheet moulding compounds. *Radiation Physics and Chemistry* 173, 108872.
9. State Committee for Standards of the USSR, 1984. Epoxy-dian resins (uncured): Technical specifications. GOST 10587–84, Moscow.
10. Jia, Y., Zhang, K., 2024. One-step synthesis of graphene/silica nanocomposites for corrosion-resistant epoxy coatings. *RSC Advances* 14(17), 11759. https://doi.org/10.1039/d4ra00529h
11. Kumar, S.S.A., Batoo, K.M., Wonnie, I.A., Ramesh, K., Sivasamy, R., Shah, M.A., 2023. GO-based polymer nanocomposite coatings with improved stability. *Scientific Reports*. https://doi.org/10.1038/s41598-023-35154-x
12. Liu, X., Chen, L., Liu, Z., Song, Q., Liu, C., 2021. Optimization of thermal and hydrophobic properties of GO-doped epoxy coatings. *Nanotechnology Reviews* 10(1), 1236. https://doi.org/10.1515/ntrev-2021-0072

13. Ramírez-Soria, E.H., León-Silva, U., Lara-Ceniceros, T.E., Advíncula, R.C., Bonilla-Cruz, J., 2022. Functionalized GO nanoplatelets for corrosion-resistant coatings. *ACS Applied Nano Materials* 5(11), 16760. https://doi.org/10.1021/acsanm.2c03276
14. Sanya, O.T., Panesar, D.K., 2026. Graphene-based nanofiller coatings for corrosion protection. *Progress in Organic Coatings* 213, 109900. https://doi.org/10.1016/j.porgcoat.2025.109900
15. Selim, M.S., El-hoshoudy, A.N., Zaki, E.G., Elsaeed, S.M., Farag, A.A., 2024. Durable graphene-based alkyd nanocomposites. *Environmental Science and Pollution Research* 31(31), 43476.
16. Thorshaug, K., Didriksen, T., Jensen, I.T., Carvalho, P.A., Yang, J., Grandcolas, M., et al., 2024. Orientation of reduced graphene oxide in coatings. *Nanoscale Advances*. https://doi.org/10.1039/d3na01057k
17. Wang, W., Jia, C., Liang, X., Wang, M., Zhao, H., 2025. Enhanced corrosion resistance of epoxy coatings with functionalized GO. *Progress in Organic Coatings* 200, 109043. https://doi.org/10.1016/j.porgcoat.2024.109043
18. Yadav, A., Panjikar, S., Raman, R.K.S., 2025. Graphene-based coatings for corrosion resistance. *Nanomaterials* 15(7), 486. https://doi.org/10.3390/nano15070486
19. Tene, T., Gahramanli, L., Muradov, M., Mammadova, A., Khudaverdiev, V., Azizova, A., et al., 2026. Hydrogen-bonded interphase in GO nanocomposites. *Frontiers in Chemistry* 13, 1710575. https://doi.org/10.3389/fchem.2025.1710575
20. Guerrero-Contreras, J., Caballero-Briones, F., 2015. Graphene oxide with different oxidation degrees via modified Hummers method. *Materials Chemistry and Physics* 153, 209–220. https://doi.org/10.1016/j.matchemphys.2015.01.005